Available online at www.sciencedirect.com
ScienceDirect
Ceramics International 36 (2010) 1339–1346
CERAMICS INTERNATIONAL
www.elsevier.com/locate/ceramint

Structural, magnetic and electrical properties of Ga-substituted NiCuZn nanocrystalline ferrite

M.A. Gabal *, S.A. Al-Thabaiti, E.H. El-Mossalamy, M. Mokhtar

Chemistry Department, Faculty of Science, King Abdul Aziz University, Jeddah, Saudi Arabia

Received 1 June 2009; received in revised form 9 November 2009; accepted 4 January 2010
Available online 29 January 2010

Abstract

In this work, we studied the substitution effect of iron by gallium on the structural, magnetic and electrical properties of the ferrite system; $Ni_{0.5}Cu_{0.25}Zn_{0.25}Fe_{2-x}Ga_xO_4$ ($x = 0$–1.0), synthesized by using the urea combustion method. XRD patterns of the samples calcined at 700 °C show only cubic spinel ferrite with an average crystallite sizes in the range of 40–54 nm. The lattice parameters were slightly changed with increasing Ga content which can be explained on the basis of the relative ionic radii of Ga^{3+} and Fe^{3+} ions. FT-IR measurements show two fundamental absorption bands, assigned to the vibration of tetrahedral and octahedral complexes, which were slightly changed with increasing Ga content. Mössbauer measurements enable us to predict the possible cation distribution of the system. It was found that Ga^{3+} ion prefer to substitute Fe^{3+} ions located in the octahedral site. Superparamagnetic state was observed in the Mössbauer spectra of the samples with Ga content >0.5. The decrease of the magnetic hyperfine field with gallium concentration was explained on the basis of supertransferred hyperfine interaction. A semiconducting behavior was inferred for all samples and the conductivity values were found to decrease with increasing the Ga content. The conduction mechanism in the spinel ferrite compounds was explained in terms of the hopping conduction process. The dielectric constant measured as a function of frequency and temperature was found to be dependent on the Ga concentration. The determined transition temperature was found to decrease with increasing Ga content.

Keywords: NiCuZn ferrite; Ga substitution; Urea combustion; XRD; Mössbauer; Conductivity; Dielectric

1. Introduction

Synthesis and application of magnetic nanoparticles with diameters of a few nanometers is a subject of intense research because of their unique properties that make them attractive, both from the scientific value of understanding their properties, and the technological significance of enhancing the performance of the existing materials [1]. In this regard, spinel ferrites, which can widely used in computer peripherals, telecommunication equipments, permanent magnets, electronic and microwave devices, are particularly important because of their thermodynamic stability, electrical conductivity, electro-catalytic activity, corrosion resistance and excellent magnetic properties which can be tailored by chemical manipulations to meet stringent requirements in various applications [2].

Up till now, Ni–Cu–Zn ferrites have been the dominant materials for multi-layer chips inductors (MLCI) due to its better electromagnetic properties at high frequency and low sintering temperature. MLCIs have recently been developed as a surface mounting device (SMT) for miniaturization of electronic devices. They are important components for the electronics products, such as cellular phone, notebook computer, video camera, etc. [3].

In MLCI applications, silver (Ag) is generally used as an internal conductor of the multi-layer ferrite chip, but as its melting point is 960.5 °C, developing a ferrite material which can be sintered at a temperature less than 950 °C and establishing a sintering technology are necessary [4].

Fu et al. [5] have been synthesized Ni–Cu–Zn ferrite powders by microwave-induced combustion process. The resultant powders, annealed at different temperature, were investigated by DTA-TG, XRD, TEM, SEM, and VSM. The as-received

* Corresponding author. Permanent address: Chemistry Department, Faculty of Science, Benha University, Benha, Egypt. Tel.: +966 557071572.
E-mail address: mgabalabdonada@yahoo.com (M.A. Gabal).

0272-8842/$36.00
doi:10.1016/j.ceramint.2010.01.021

powders showed the formation of cubic ferrite with a saturation magnetization (M_s) of 63 emu/g. The M_s increased to 75 emu/g for the sample annealed at 700 °C for 2 h.

Su et al. [6] investigated the effects of composition and sintering temperature on grain size, porosity and magnetic properties of NiCuZn ferrites prepared by conventional ceramic method.

Ni–Cu–Zn ferrites [7] have been synthesized by employing co-precipitation technique using oxalate precursors. X-ray diffractograms show single-phase formation. The lattice parameters were found to decrease with the addition of Ni^{2+} which is attributed to smaller ionic sizes of Ni^{2+}, which replaces Cu^{2+}. The initial permeability shows an increase up to a certain concentration of Ni^{2+} then decreases.

The ferrite compositions $Ni_{0.8-x}Cu_{0.2}Zn_xFe_2O_4$ with $x = 0.5$, 0.55 and 0.6, were synthesized [8] through nitrate–citrate gel auto-combustion method. The ferrite was characterized using X-ray diffraction. As-burnt powders showed the presence of crystalline cubic spinel ferrite with about 19–22 nm. The sintered ferrite was characterized for permeability, saturation magnetization, relative loss and ac resistivity measurements.

A nitrate–citrate gel was prepared [9] from metal nitrates and citric acid by sol–gel process, in order to synthesize $Ni_{0.25}Cu_{0.25}Zn_{0.50}Fe_2O_4$ ferrite. The sintered ferrite possesses fine-grained microstructure, good frequency stability and high-quality factor compared to the sample prepared by conventional ceramic route.

Generally, the basic properties of NiCuZn ferrites, depending on the applications of interest, can be improved by substituting or adding various ions of different valence states [10,11]. Roy and Bera [12] found that, the substitution of nickel with magnesium in $Ni_{0.25-x}Mg_xCu_{0.2}Zn_{0.55}Fe_2O_4$ (with $x = 0.18$), synthesized using nitrate–citrate auto-combustion method, results in the improvement of the electromagnetic properties, through lowering magnetostriction constant and increasing resistivity.

The effects of CuO and V_2O_5 additions and the particle sizes of the precursor materials on the microstructure and relative initial permeability of low firing temperature NiCuZn ferrites were investigated [13].

The mixing of $(Ni_{0.38}Cu_{0.12}Zn_{0.50})Fe_2O_4$ powders with Bi_2O_3 was performed using solid-state mixing as well as wet chemical coating processes such as ammonia precipitation coating, urea precipitation coating, and solution coating [14]. Ferrites with 1.5 wt% Bi_2O_3 addition by ammonia precipitation coating sintered at 900 °C can provide the best permeability and quality factor among all the cases studied.

The present work reports the preparation procedures and the results of XRD, FT-IR and Mössbauer studies of $Ni_{0.5}Cu_{0.25}Zn_{0.25}Fe_{2-x}Ga_xO_4$ system ($x = 0$–1.0). Our aim is to shed more lights on crystallographic structure in these diluted ferrimagnets. Besides, the studying of the changes in the electrical and magnetic properties of the investigated system upon the addition of Ga^{3+} ions will be of great importance. Currently, there is no any work in the literature on the diamagnetic substitution of NiCuZn ferrite using Ga^{3+} ions.

2. Experimental procedure

2.1. Preparation method

$Ni_{0.5}Cu_{0.25}Zn_{0.25}Fe_{2-x}Ga_xO_4$ system ($x = 0$–1.0) will be prepared through the urea combustion reaction [15]. Urea is used as fuel and stoichiometric amounts of $Ni(NO_3)_2{\cdot}6H_2O$, $Cu(NO_3)_2{\cdot}3H_2O$, $Zn(NO_3)_2{\cdot}6H_2O$, $Fe(NO_3)_3{\cdot}9H_2O$ and $Ga(NO_3)_3{\cdot}7H_2O$ were used as cation precursors. It is well known that the stoichiometric mole ratio of urea needed to balance the total oxidizing and reducing valencies, and to release the maximum energy for the reaction in the mixture of oxidizer and fuel in ferrite materials is 6.67.

The reactants were dissolved in a minimum quantity of distilled water in a Pyrex beaker. The mixture was then placed on a hot plate magnetic stirrer maintained at around 400 °C. Initially the solution boiled and underwent dehydration followed by decomposition with evolution of copious amounts of heat and gases. The mixture was then frothed and swelled forming foam, which ruptured with a flame and finally gave foamy powder of the products.

The as-burnt ferrites were then calcined in an electrical furnace under static air atmosphere at 500 or 700 °C for 2 h. The samples were then air-quenched to room temperature and stored in a desiccator.

2.2. Techniques

X-ray powder diffraction measurements were obtained using a D8 Advanced diffractometer (Bruker AXS, Germany) at ambient temperature using monochromated Cu $K_{\alpha 1}$ radiation ($\lambda = 1.5406$ Å).

Fourier transform-infrared spectra were recorded at room temperature in the frequency range of 1000–200 cm^{-1}, employing KBr disc technique, using a Jasco FT-IR 310 spectrophotometer.

Austin Science Mössbauer Spectrometer with constant acceleration laser-interferometer-controlled drive was used in a standard transmission setup with a Personal Computer Analyzer (PCA II-card with 1024 channels). The radioactive source is ^{57}Co imbedded in Rh matrix with initial activity of 50 mCi. Metallic iron spectrum was used for the calibration of hyperfine magnetic fields. The absorber thickness is approximately 10 mg cm^{-2} of natural iron. Experimental data were analyzed using the least-square fitting ‘‘Mos-90’’ computer program [16].

For electrical properties measurements, the ferrite samples in a powdered form were compressed to pellets of 1 cm diameter and about 1 mm thickness. The applied pressure was 2 tons cm^{-2}. Pellets of the samples were then annealed at 900 °C for 2 h and cooled to room temperature. The two surfaces of each pellet were polished and coated with silver paint and tested for Ohmic contact. The real part of the dielectric constant (ε') and ac conductivity were measured, by a Hioki LCR bridge model 3531 (Japan) using the two-probe method [17], at different frequencies (10–1000 kHz) as a function of temperature. The temperature of the sample was

measured using a thermocouple type K which is connected to a digital thermometer.

3. Results and discussion

3.1. Characterization of Ga-substituted NiCuZn ferrites

3.1.1. X-ray diffraction

X-ray powder diffraction studies (XRD) have been carried out on the as-burnt powders, samples calcined at 500 °C or at 700 °C for 2 h.

Fig. 1 shows XRD patterns of the as-burnt samples. From the figure it is clear that, the samples with $x \leq 0.1$ show XRD patterns of low crystallinity with peaks positions indicate the formation of ferrites. This means that these ferrites can be directly formed after the auto-combustion reaction. The presence of secondary phases of Fe_2O_3 (hematite, JCPDF 89-0598) and Ga_2O_3 (hematite, JCPDF 43-1012), having very low intensive peaks, were also observed. The enlarged diffraction line of these samples demonstrates their nanometric nature. The average crystallite size estimated using Scherrer formula [18] for these samples are 12 and 43 nm, respectively.

The increase in the gallium content ($x > 0.1$) generally causes the intensity of the characteristic peaks of the ferrite phase to decrease and gave nearly amorphous patterns except for the sample with $x = 0.7$ which shows well crystalline intensive peaks with an average crystallite size of 50 nm. This indicates that the addition of gallium reduces the crystallinity of the ferrite phase. This may be attributed to the fact that higher concentrations of gallium reduce the flame combustion temperature, which directly affects the formation and crystallinity of the phase [19]. The presence of a secondary phase is still detectable in these samples instead of their low crystallinity. The gallium content of 0.7 can be considered as the critical gallium concentration.

XRD of the samples calcined at 500 °C are represented in Fig. 2. The figure reflects the decrease in the amorphous nature of the samples. The intensities of the peaks attributed to the secondary phases were accordingly increased which indicates the incomplete solid reactions at this stage.

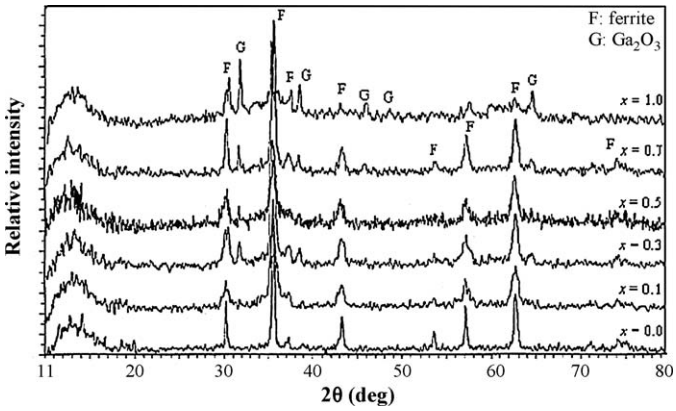

Fig. 2. Characteristic parts of XRD patterns of $Ni_{0.5}Cu_{0.25}Zn_{0.25}Fe_{2-x}Ga_xO_4$ system calcined at 500 °C.

For the sample calcined at 700 °C, the X-ray diffraction patterns at all the compositions (Fig. 3) showed sharp and intensive peaks characteristic for single cubic spinel phase. The average crystallite size and lattice parameter of sintered ferrites at 700 °C are shown in Table 1 along with their bulk density. The samples show an average crystallite sizes in the range of 40–54 nm which indicates that the synthesized ferrites have nano-sized crystallites.

From the table it is obvious that, the lattice parameters are slightly changed with increasing Ga content. This can be explained on the basis of the relative ionic radii of Ga^{3+} and Fe^{3+} ions. The ionic radius of Ga^{3+} (0.62 Å) is nearly the same like that of Fe^{3+} in the octahedral site (0.645 Å) and consequently, the partial replacement of the latter by the former causes very small changes in the unit cell dimensions.

The X-ray density (D_x), can be calculated using the relation: $D_x = ZM/Na^3$; where Z is the number of molecules per unit cell ($Z = 8$), M is the molecular weight, N is Avogadro's number and a^3 is the volume of unit cell [18]. It was found that, X-ray density increases with increasing Ga content. This increase was expected since the Ga atom is heavier than the iron atom, and this increase in weight with nearly constant size of both atoms causes an increase in the X-ray density.

From XRD study it is obvious that, the nano-sized Ga-substituted NiCuZn ferrites, which usually forms at high

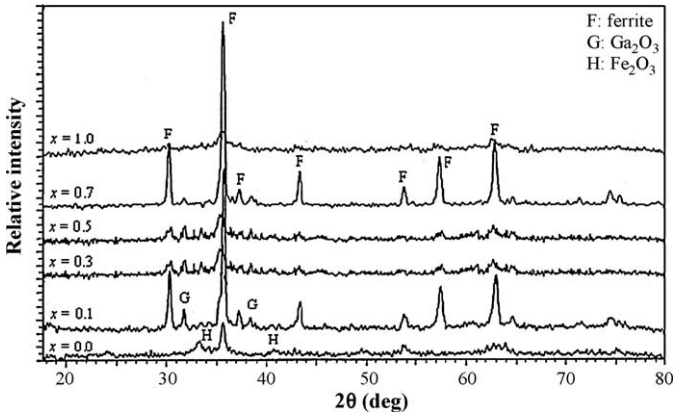

Fig. 1. Characteristic parts of XRD patterns of $Ni_{0.5}Cu_{0.25}Zn_{0.25}Fe_{2-x}Ga_xO_4$ as-burnt system.

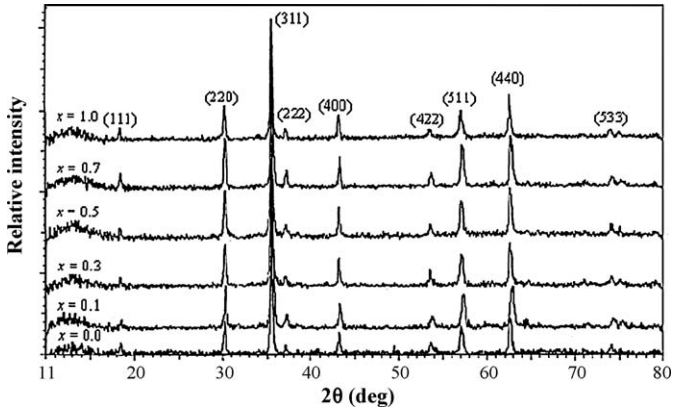

Fig. 3. Characteristic parts of XRD patterns of $Ni_{0.5}Cu_{0.25}Zn_{0.25}Fe_{2-x}Ga_xO_4$ system calcined at 700 °C.

Table 1
Lattice parameters, X-ray densities, average crystallite size and FT-IR spectral data of $Ni_{0.5}Cu_{0.25}Zn_{0.25}Fe_{2-x}Ga_xO_4$ system.

Ga content, x	Lattice parameter (Å)	D_x (gm cm^{-3})	Average crystallite size (nm)	ν_1 (cm^{-1})	ν_2 (cm^{-1})
0.0	8.3705	5.3736	49	398	582
0.1	8.3464	5.4520	40	400	589
0.3	8.3706	5.4676	43	398	582
0.5	8.3642	5.5433	45	398	583
0.7	8.3504	5.6340	54	394	582
1.0	8.3704	5.6879	50	396	581

temperatures in conventional method, has been completely formed at 700 °C during combustion synthesis and subsequent heat-treatment.

3.1.2. FT-IR measurements

Fig. 4 shows FT-IR spectra of the samples calcined at 700 °C in the frequency range of 1000–200 cm^{-1}.

Two main broad metal–oxygen bands are seen in the IR spectra of all spinels, and ferrites in particular. Waldron [20] attributed the band ν_1 at around 600 cm^{-1} to the intrinsic vibration of tetrahedral metal oxygen complexes and the band ν_2 at around 400 cm^{-1} to the intrinsic vibration of octahedral metal oxygen complexes. The results of FT-IR spectroscopic measurements obtained in the present work are summarized in Table 1.

From the table it is clear that the values of ν_1 and ν_2 are slightly changed with the Ga substitution. This attributed again to the nearly equal ionic radii of both Ga^{3+} and Fe^{3+} ions.

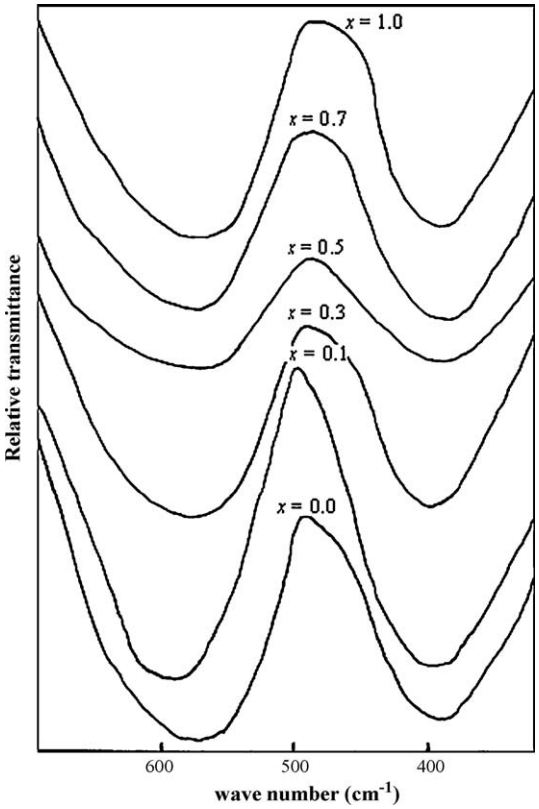

Fig. 4. FT-IR spectra of $Ni_{0.5}Cu_{0.25}Zn_{0.25}Fe_{2-x}Ga_xO_4$ system calcined at 700 °C.

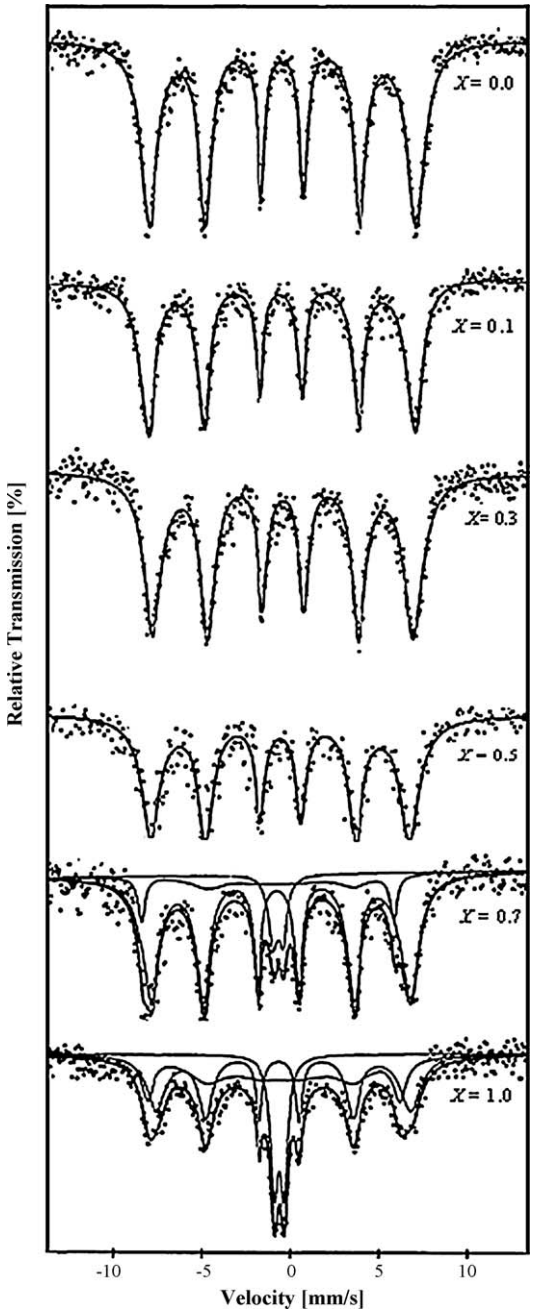

Fig. 5. The Mössbauer spectra at room temperature of $Ni_{0.5}Cu_{0.25}Zn_{0.25}Fe_{2-x}Ga_xO_4$ system.

Table 2
Mössbauer parameters of $Ni_{0.5}Cu_{0.25}Zn_{0.25}Fe_{2-x}Ga_xO_4$ system.

Ga content, x	Site	Isomer shift, δ ($\pm$0.02 mm s^{-1})	Quadrupole splitting, ΔE_Q ($\pm$0.02 mm s^{-1})	Line width, Γ (mm s^{-1})	Hyperfine field, H_n ($\pm$2 kOe)
0.0	B	0.355	−0.009	0.439	472
0.1	B	0.412	−0.019	0.478	469
0.3	B	0.423	−0.021	0.591	457
0.5	B	0.495	−0.026	0.609	452
0.7	A	0.328	−0.74	4.480	436
	B	0.423	0.098	0.144	447
1.0	A	0.323	−0.358	4.610	438
	B	0.485	0.236	0.311	435

3.1.3. Mössbauer studies

Typical Mössbauer spectra of the $Ni_{0.5}Cu_{0.25}Zn_{0.25}Fe_{2-x}Ga_xO_4$ system, taken in zero applied magnetic fields at room temperature are represented in Fig. 5. The experimental data were analyzed with a standard least-square fitting program assuming Lorentzian line shapes. The Mössbauer solid lines for the samples were fitted using sextets, which can be ascribed to Fe^{3+} ions in A- and B-sites according to the values of magnetic hyperfine field, and doublet representing paramagnetic or super paramagnetic behavior. The characteristic parameters of Mössbauer spectra including hyperfine field (H_n), isomer shift (δ), quadrupole splitting (ΔE_Q), and line width (Γ) are summarized in Table 2.

Basing on the site-preference energy data and the Mössbauer effect results [21], Zn^{2+} ions are preferentially occupying A-sites while Ni^{2+} and Cu^{2+} ions have the tendency to occupy the B-sites in the spinel unit cell. The present preparation method may have a great effect on the cation distribution by which these ions preferred the normal spinel. Mahmoud [22] reported that Ga substitutes Fe at the tetrahedral A-site in the spinel ferrite unit cell. On the other hand Ata-Allah [21] recently reported that Ga substitutes for Fe at the octahedral B-site in this unit cell.

The Mössbauer spectra of the samples with $0.0 \leq x \leq 0.5$ show a broad magnetically split spectrum attributed to a ferromagnetic component. The spectra are fitted into one sextet due to Fe^{3+} ions at the B-site which indicates that, Ga^{3+} ions are preferred to occupy the octahedral B-site. The cation distribution in these samples can be deduced as: $(Zn_{0.25}Cu_{0.25}Ni_{0.5})[Ga_xFe_{2-x}]O_4$.

For the samples with $x > 0.5$ the spectra show a substantial central doublet besides contributions from a broad magnetically split spectral component. The development of a quadrupole doublet in Mössbauer spectra is an indication of superparamagnetism [23]. The presence of both quadrupole split and magnetic split spectra components is characteristic of nanograined materials and according to Stroink et al. [24] the relative proportions of the two components can yield information about the grain size distribution. The magnetic spectrum consists of two clearly splitted Zeeman sextets due to Fe^{3+} at tetrahedral and octahedral sites. The fraction of iron at the two distinct crystallographic sites can be determined by knowing the area under the resonance lines due to these ions.

As it can be noticed from the spectrum for $x = 0.7$, the A-site peaks start to appear with smaller area ratio relative to B-site peaks. This distribution of Fe^{3+} ions among the two crystallographic sites will results in the migration of some Ni^{2+} ions from tetrahedral site to the octahedral site to balance the cationic distribution. Increasing the Ga content to 1.0, will result in a successive increase in the ratio of the A-site peaks, this means more transfer of Fe^{3+} ions from B-site to A-site. Consequently, based on these Mössbauer spectra and the area under these two resonance lines, the possible ionic distribution of the samples with $x > 0.5$ can be represented as: $(Zn_{0.25}Cu_{0.25}Ni_{(0.5-y)}Fe_y)[Ni_yGa_xFe_{2-x-y}]O_4$. The relative

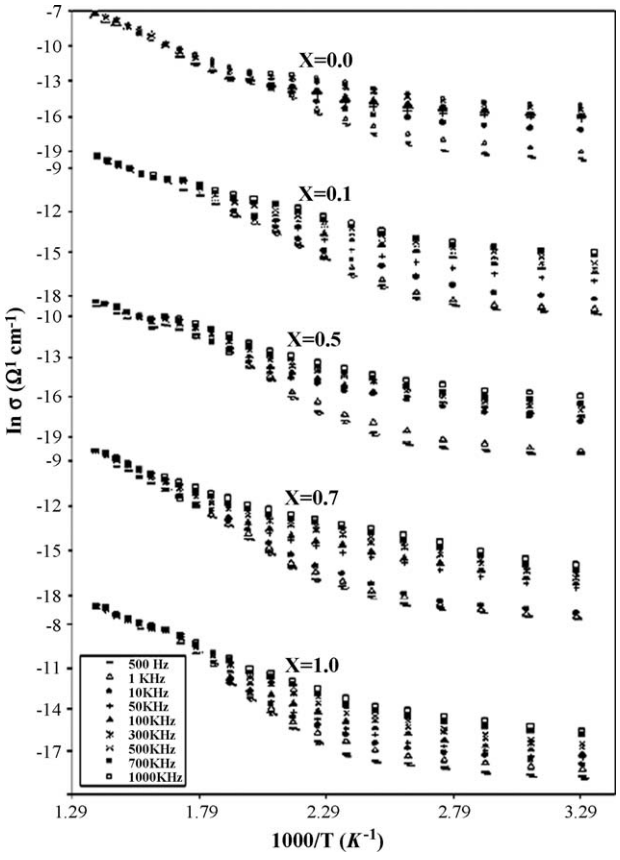

Fig. 6. Relation between $\ln \sigma$ and reciprocal of absolute temperature at different Ga content as a function of applied frequency for $Ni_{0.5}Cu_{0.25}Zn_{0.25}Fe_{2-x}Ga_xO_4$ system.

increase in the quadrupole doublet with increasing Ga content can be ascribed to the increase in superparamagnetism.

Generally, the decrease in the measured magnetic hyperfine field at both sites with increasing the gallium content suggested to be just a decrease in the supertransferred hyperfine field when the diamagnetic Ga^{3+} ions ($3d^{10}$) replace the magnetic Fe^{3+} ion ($3d^5$). Also it is clear from the Mössbauer spectra that increasing Ga content reveals a relaxation process, which is clearly observed from the increase of the peaks line width (Table 2). This is due to the substitution of Ga may isolate some magnetic domains at the octahedral B-site in the spinel unit cell and raise the height of the energy barriers and in turn increase the relaxation effect. The change in the isomer shift and quadrupole splitting values can be interpreted by the change of local environments of B-sites Fe^{3+} ions as the amount of Ga^{3+} ions increases.

3.1.4. Electrical properties studies

The electrical conductivity is an important property of low temperature sintered ferrite for MLCI application. Fig. 6 shows typical curves correlates the ac conductivity ($\ln \sigma$) and the reciprocal of absolute temperature ($1000\,T^{-1}$), for $Ni_{0.5}Cu_{0.25}Zn_{0.25}Fe_{2-x}Ga_xO_4$ system, in the frequency range from 500 Hz to 1 MHz.

It can be noticed that, the conductivity increases with increasing temperature in a semiconducting behavior. The linear relation was broken to three lines at two temperatures, indicated as three temperature ranges. This change in the slope of the straight line is related to the change in the conduction mechanism accompanied by transformation from the ferrimagnetic to paramagnetic state at Curie point and the magnetic phase transition in ferrimagnetic state [10]. The magnitude of the slope depends on the exchange interaction between the outer and inner electrons, which changes at the Curie temperature and the magnetic phase transition temperature.

In the first region, the conductivity is strongly dependent on frequency but is weakly temperature dependent. In this region, the thermal energy is not enough to liberate charge carriers and consequently the conductivity is hardly changed with temperature. In the intermediate temperature region (ferrimagnetic region), a temperature dependence and weak frequency dependence is observed. In the high temperature region (paramagnetic region), strong temperature dependence appeared. The increase in the electrical conductivity as temperature increases may be related to the increase in drift mobility of the thermally activated charge carriers (electron and hole) according to hopping conduction mechanism.

The samples show an anomalie at intermediate temperatures. Such behavior is similar to that reported previously for other ferrite system [25], where a minute change in the slope at the Néel point was remarked. One of the possible explanations of this anomaly is the substitution of gallium in place of iron in the unit cell which increases the activation energy due to the completely filled Ga^{3+} d-orbitals which have much lower energy and being more contracted than the Fe^{3+} orbitals. Also, the decreased overlap of Ga^{3+} d-orbitals with oxygen 2p-orbitals has an indirect but appreciable effect on hopping conduction at octahedral sites.

Table 3
Values of conductivities and activation energies at applied frequency of 100 kHz for $Ni_{0.5}Cu_{0.25}Zn_{0.25}Fe_{2-x}Ga_xO_4$ system.

Ga content, x	σ at 343 K (Ω^{-1} cm^{-1})	Activation energy (eV)		T_d (K)
		E_f	E_p	
0.0	2.3×10^{-7}	0.19	0.40	603
0.1	1.7×10^{-7}	0.20	0.46	596
0.5	5.6×10^{-8}	0.26	0.51	491
0.7	5.0×10^{-8}	0.28	0.57	585
1.0	4.6×0^{-8}	0.33	0.61	576

From Fig. 6 it is obvious that, the conductivity values taken at 343 K and a frequency of 100 kHz (Table 3) are in the range meeting the requirement of MLCIs [26].

The conductivity values were found to decrease with increasing the Ga content. This decrease can be attributed to the decrease in the total number of charge carriers. The conduction mechanism in the spinel ferrite compounds can be explained in terms of the hopping conduction process which occurs among Fe^{2+} and Fe^{3+} in the octahedral B-sites. It is known that the formation of Fe^{2+} may be expected owing to the partial reduction of Fe^{3+} to Fe^{2+} and evaporation of Zn ions during the sintering process [12]. One can observe that the composition changes induced by partial substitution of Fe^{3+} with Ga^{3+} have different influences on the electrical conductivity because gallium exists exclusively as Ga^{3+}, its presence in the ferrite lattice avoids the appearance of Fe^{2+} ions and the number of the electronic jumps between Fe^{2+} and Fe^{3+} ions will decrease. Moreover, the porous structure of Ga doped ferrite impedes the motion of charge carriers [27].

It can be also observed from Fig. 6 that the AC conductivity increases with increasing applied frequency. Since the increase in frequency enhances the hopping frequency of the charge carriers Fe^{2+} and Fe^{3+}, the conduction is increased.

The compositional dependence of the activation energy evaluated from the slopes of the linear plots of electrical conductivity in the ferrimagnetic and paramagnetic ranges is shown in Table 3. The general trend of the activation energy, in both regions, is to be increased with increasing gallium concentration, which means a decrease in the mobility of charge carriers. The activation energy for the electric conduction in the paramagnetic region (E_p) was found to be higher than that for the ferrimagnetic region (E_f). This could be attributed to the disordered states of the former region and the ordered states of the latter region. The most predominant mechanism of conduction in the low temperature region is the hopping of electrons between the ions of different valances. Accordingly, small activation energy for this region is obtained. The large activation energy of the high temperature region indicates that the conduction is mainly due to a small positive polarons which migrate inside the sample under the effect of the large thermal energy due to heating and small internal viscosity of the sample.

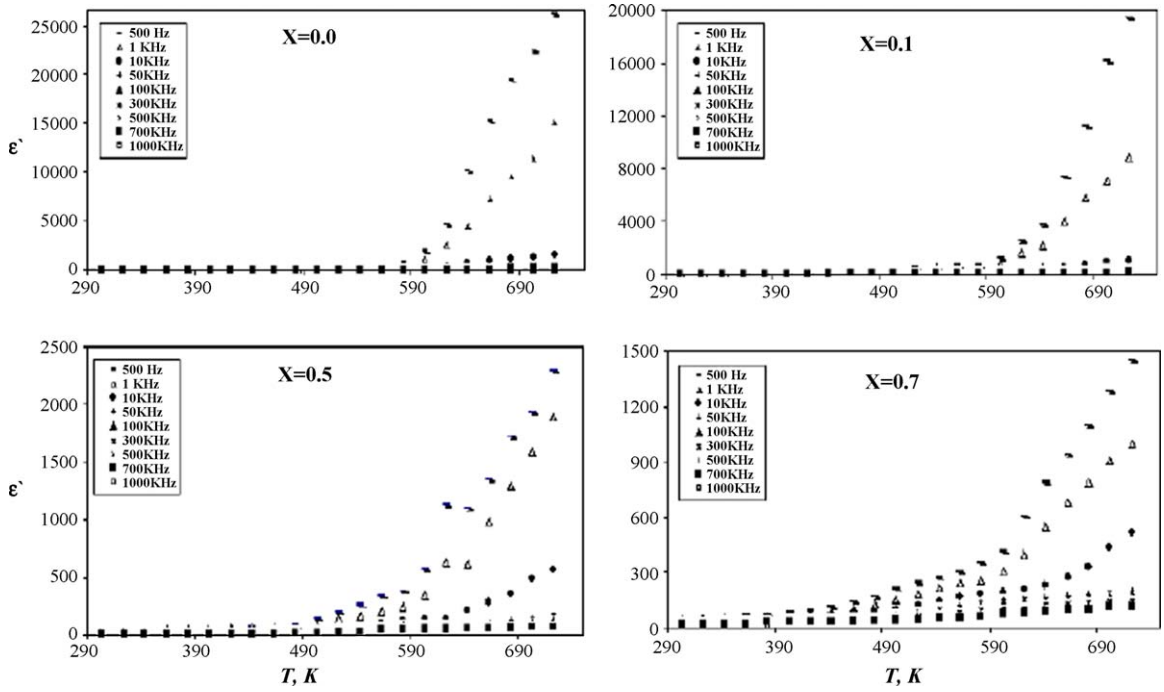

Fig. 7. Relation between dielectric constant and the absolute temperature as a function of applied frequency for $Ni_{0.5}Cu_{0.25}Zn_{0.25}Fe_{2-x}Ga_xO_4$ system.

The dielectric property, such as dielectric constant, is also of importance for MLCIs, especially for devices used in high frequency range. The relation of the real part of dielectric constant (ε') as a function of temperature at different frequency for $Ni_{0.5}Cu_{0.25}Zn_{0.25}Fe_{2-x}Ga_xO_4$ system is illustrated in Fig. 7. The relation shows a sensitive dependence of ε' on both frequency and temperature as a function of compositional parameter x. The dependence of ε' on frequency or temperature is very small at low temperatures. The dielectric constant was found to decrease with increasing in frequency for all the samples which can be considered as a normal dielectric behavior [30]. Increasing the temperature will increase this dependence. There are also, abrupt changes in this relation indicating a phase transition at temperatures 603, 596, 591, 585 and 576 K for $x = 0.0$, 0.1, 0.5, 0.7 and 1.0, respectively as shown in Fig. 7. These values of the transition temperature are in good agreement with that obtained from the AC electrical conductivity measurements of these materials (Fig. 6). These changes are accompanied with the phase transformation from the ferrimagnetic (ordered) state to the paramagnetic (disordered) state. The decrease in the transition temperature (T_d) with increase in the Ga content agrees with Gilleo studies for superexchange interaction for various oxides [28], which indicated that Curie temperature depends primarily upon the number of Fe^{3+}–O^{2-}–Fe^{3+} linkages. Replacing Fe with Ga in the B-site decrease the number of Fe^{3+}–O^{2-}–Fe^{3+} linkages and therefore the transition temperature [29].

4. Conclusion

Nano-sized cubic ferrites of composition $Ni_{0.5}Cu_{0.25}Zn_{0.25}Fe_{2-x}Ga_xO_4$ ($0.0 \leq x \leq 1.0$) were successively prepared through urea combustion method. The lattice parameters were slightly changed with increasing Ga content while, X-ray density increases. The FT-IR patterns show the characteristic peaks of ferrite system. Mössbauer spectroscopy showed that Ga^{3+} ions prefer to substitute Fe^{3+} ions located in the octahedral site. Superparamagnetic state is observed in the Mössbauer spectra of the samples with Ga content >0.5. The decrease in the magnetic hyperfine interaction at the A- and B-sites is explained by the decrease in the supertransferred hyperfine field when Ga^{3+} ions replace Fe^{3+} ions. Semiconducting behavior is inferred for all samples and the conductivity values were found to decrease with increasing the Ga content due to the decrease in the total number of charge carriers. The dielectric constant is found to be strongly dependent on temperature and frequency. The determined transition temperature is found to decrease with increasing Ga content.

Acknowledgement

The Investigators are grateful to King Abdul Aziz University, Jeddah, KSA for providing financial support for this work (Project No. N 153/427).

References

[1] D. Fiorani, in: J.L. Dormann, D. Fiorani (Eds.), Magnetic Properties of Fine Particles, North Holland Delta Series, 1992.
[2] Q. Chen, Z.J. Zhang, Appl. Phys. Lett. 73 (1998) 3156.
[3] Z. Yue, L. Li, J. Zhou, H. Zhang, Z. Ma, Z. Gui, Mater. Lett. 44 (2000) 279.
[4] J.H. Jean, C.H. Lee, W.S. Kou, J. Am. Ceram. Soc. 82 (1999) 343.
[5] Y. Fu, C. Lin, C. Liu, J. Magn. Magn. Mater. 283 (2004) 59.
[6] H. Su, H. Zhang, X. Tang, Y. Jing, Y. Liu, J. Magn. Magn. Mater. 310 (2007) 17.

[7] S.A. Ghodake, U.R. Ghodake, S.R. Sawant, S.S. Suryavanshi, P.P. Bakare, J. Magn. Magn. Mater. 305 (2006) 110.
[8] P.K. Roy, J. Bera, J. Mater. Process. Technol. 197 (2008) 279.
[9] Z. Yue, J. Zhou, L. Li, H. Zhang, Z. Gui, J. Magn. Magn. Mater. 208 (2000) 55.
[10] Z. Yue, J. Zhou, Z. Gui, L. Li, J. Magn. Magn. Mater. 264 (2003) 258.
[11] Y. Fu, K. Pan, C. Lin, Mater. Lett. 57 (2002) 291.
[12] P.K. Roy, J. Bera, J. Magn. Magn. Mater. 298 (2006) 38.
[13] M. Yan, J. Hu, W. Luo, W. Zhang, J. Magn. Magn. Mater. 303 (2006) 249.
[14] S. Wang, Y. Wang, T. Yang, C. Chen, C. Lu, C. Huang, J. Magn. Magn. Mater. 220 (2000) 129.
[15] A. Junior, E. Lima, M. Novak, P. Wells, J. Magn. Magn. Mater. 308 (2007) 198.
[16] G. Grosse, Mos-90, Version 2.2, 2nd ed., Oskar-Maria-Graf-Ring, Munchen, 1992.
[17] K.V. Kumar, D. Ravindar, Mater. Lett. 52 (2002) 166.
[18] B.D. Culity, Elements of X-ray Diffraction, vol. 99, Addison-Wesley, Reading, MA, 1967.
[19] A. Costa, A. Diniz, A. Melo, R. Kiminami, D. Cornejo, A. Costa, L. Gama, J. Magn. Magn. Mater. 320 (2008) 742.
[20] R.D. Waldron, Phys. Rev. 99 (1955) 1727.
[21] S.S. Ata-Allah, J. Magn. Magn. Mater. 284 (2004) 227.
[22] M.A. Mahmoud, Solid State Commun. 120 (2001) 451.
[23] S.S. Ata-Allah, A. Hashhash, J. Magn. Magn. Mater. 307 (2006) 191.
[24] G. Stroink, D. Lim, R.A. Dunlap, Phys. Med. Biol. 32 (1987) 203.
[25] M.K. Fayek, M.F. Mostafa, F. Sayedahmed, S.S. Ata-Allah, M. Kaiser, J. Magn. Magn. Mater. 210 (2000) 189.
[26] Z. Yue, J. Zhou, L. Li, Z. Gui, J. Magn. Magn. Mater. 233 (2001) 224.
[27] E. Rezlescu, N. Rezlescu, F. Tudorache, P.D. Popa, J. Magn. Magn. Mater. 272–276 (2004) 1821.
[28] M.A. Gilleo, Phys. Chem. Solids 13 (1960) 33.
[29] S.S. Ata-Allah, M.K. Fayek, H.A. Sayed, M. Yehia, Mater. Chem. Phys. 92 (2005) 278.
[30] M. Kaiser, Phys. Status Solidi (a) 201 (2004) 3148.